A Multicriteria Optimisation Design of SPSE for Adaptive LEO Satellites Missions Using the PSI Method

Sunday C. Ekpo[1] and Bamidele Adebisi[2]

Manchester Metropolitan University, Manchester, Greater Manchester, M1 5GD, United Kingdom

and

Danielle George[3]
The University of Manchester, Manchester, Greater Manchester, M60 1QD, United Kingdom

The spacecraft power system engineering (SPSE) analysis for the radiation-prone space environment is a major critical satellite engineering definition for realising successful mission and post-mission capabilities. The dynamic operations and post-mission applications of capability-based small satellites require an adaptive architecture(s) which exhibits an enormous conceptual system engineering design task in terms of the trade space – which can be too large to explore, study, analyse and qualify – for a reliable and sustainable mission. This paper involves a multicriteria optimisation design of the SPSE subsystems for adaptive LEO satellites missions using the parameter space investigation (PSI) method. A three-axis stabilised 10-kg nanosatellite is considered for a meteorological spacecraft (METSAT) mission at 800 km altitude. The initial case study SE parameters considered include the required payload power and spacecraft power and mass contingencies. The PSI method allows for a large-scale multicriteria optimisation of dynamic engineering systems. This was implemented in the multicriteria optimisation and vector investigation (MOVI) software. Specific power profiles for LEO satellites were used for the mathematical modelling of the highly adaptive nanosatellite (HAN) system in LEO. In the multicriteria optimisation process, 2765 design vectors entered the test table out of which 2762 formed the feasible solutions set. The PSI was conservatively designed to yield 10 pareto optimal solutions; a pareto optimal solution of 12.36 W for the payload subsystem yielded HAN mass and power margins of 1.84 kg and 2.37 W respectively. From the analysis, the solar array capability was found to deliver 24.23 W for the mission; this forms the beginning-of-life design point. The actual on-orbit mass of the HAN system (with enhanced capabilities including post-mission reuse) was found to be 9.2 kg as opposed to a conventional 10-kg nanosat implementation. The findings serve to eliminate undue space-borne equipment oversizing and advance the state-of-the-art in the conceptual design of future-generations spacecraft at the subsystem and system levels. Adaptive space systems promise to enable capability-based, dynamic, cost-effective, reliable, multifunctional, multipurpose and optimal-performing space systems with recourse to post-mission re-applications. Furthermore, the PSI-MO results show that HASS architectures can be extended to implement higher satellite generation missions with economies of scale.

Nomenclature

β   =   Sun-orbit-plane angle, º

---

[1]Research Associate, Electrical & Electronic Engineering, RM 313a, JD Building (East), *MAIAA*.
[2]Lecturer, Electrical & Electronic Engineering, RM 331 JD Building (East).
[3]Reader, Electrical & Electronic Engineering, RM 13b, Sackville Street Building.

C_f	=	contingency factor
E_o	=	the energy production of the solar panel during an orbital period, J
H_{sat}	=	altitude of the satellite, km
M	=	mass of a spacecraft, kg
P_{cb}	=	power consumption of the core bus module, W
P_{margin}	=	power margin or contingency for the spacecraft mission, W
P_p	=	power consumption of the payload processing-overpower mode, W
P_{pl}	=	power consumption of the payload module, W
P_s	=	power consumption of the power-storing mode, W
P_{sp}	=	sunlit power generation of solar panels, W
P_T	=	total power consumption of the spacecraft in orbit, W
R	=	the radius ratio
R_{eq}	=	mean equatorial radius of the Earth, km
R_{sat}	=	geocentric radius of the satellite, km
t_e	=	eclipse time of spacecraft, s
τ_o	=	orbital period of the satellite, s
μ	=	gravitational constant of the Earth, km^3/s^2

I. Introduction

THE increasing adoption and development of adaptive space systems for reconfigurable and real-time applications in space missions have necessitated the corresponding design, development and validation of the critical mission resources. Power and/or energy generation for spacecraft in orbits is based on the subsystem requirements. For highly adaptive small spacecraft (HASS)[1–3] and the conventional small satellites, the electrical power is at a premium.[4–12] Due to the size (volume), weight, shape and power limitations imposed on small satellites, it is vital for spacecraft system engineers to understand and appropriate the relevant power budget model that would guarantee a mission's success cost-effectively.

Adaptive Small satellite missions operating in the low Earth orbit (LEO) have been the bane of current global interest and hence, the existing system engineering margins are insufficient to objectively address the missions' options. CubeSats in the 1U (one unit; 10 cm x 10 cm x 10 cm; 1 kg), 2U (two unit; 10 cm x 10 cm x 20 cm; 2 kg) and 3U (three unit; 10 cm x 10 cm x 10 cm; 3 kg) categories have attracted unprecedented research interests amongst the academia, spin-off companies, space research organisations and nations with partially-funded space programmes.[1,6,7] Appropriate SE procedures that validate the mission capabilities with recourse to post-mission reuse are required. Current missions have heavily depended upon commercial-of-the-shelf (COTS) subsubsystems and subsystems for their prototyping, development construction. The low-cost benefits of using these devices are often outweighed by the inherent reliability concerns and failures of the components in space. The space environment presents a unique challenge to mission's success in that it is radiation-prone and this impacts onboard electronics and consequently the power generation, operation and design lifetime of the spacecraft.

Achieving a maximum operational and processing time by the payload module onboard a satellite is one of the critical design considerations spacecraft designers must validate prior to launch. Hence, the static and dynamic power requirements of the passive, active and adaptive components and subsystems onboard a satellite must be estimated. Furthermore, a knowledge of their respective operational times would enable a judicious development of a balanced energy budget for the current and emergent missions.

Orbital patterns[4–6,] influence the power generation probability of solar panels and hence, the batteries' stored energy reserve. This usually translates into enabling the spacecraft to operate in different cost-effective and energy-efficient multiple power modes with recourse to performance trade-offs during an orbital period.

Space-based payload data capturing and processing, mission data downlink and engineering data uplink represent the major spacecraft's in-orbit operation phases the spacecraft systems engineer must carefully and objectively qualify and quantify.[1,4,13–15] For adaptive space subsystems and components, the static power consumption is less than its dynamic counterpart. A payload module that utilises field programmable gates array (FPGA) in its architecture experiences various power consumption regimes based on the prevailing power mode(s) in the course of the spacecraft mission.[7–9] This is also true for a command and data handling subsystem that processes mission data using FPGA-based processors. For small satellites in LEO, accomplishing the mission largely depends on the energy generation capacity and reserve margin possible during a single orbital period and/or round-trip. The increase in the use of radiation-hardened FPGAs in space missions has been occasioned by its circuit-emulating hardware functionalities and/or software implementation of reconfigurable custom hardware

architectures in real-time. Moreover, onboard mission data processing and handling are performed to reduce the subsystem and functional requirements of the communication subsystem. Transmitting unprocessed data to a ground station usually demands more communication subsubsystem and subsystem resources which may not be feasible for small satellites by virtue of their limited size, weight and power. The implementation of high-speed data processing using adaptive device architectures would greatly enhance the data rate, bandwidth, availability and reliability of the communication subsystem. For instance, current medium and large satellites utilise FPGAs for computationally-intensive data processing spanning hyperspectral image, audio/sound and video processings. Traditional microprocessors have been outperformed by FPGAs in implementing data processing algorithms. A Virtex-4 SX35 FPGA device has implemented a hyperspectral imaging data processing algorithm within 15x less than the time required by a PowerPC 7455 microprocessor.[6]

In an actual satellite mission, at least two basic power modes[6] are feasible: a power-storing and an overpower modes. The total satellite system's power requirement is greater in the overpower mode (OM) than in the power-storing mode (PSM). In the OM, the sunlit solar power generation/production for the spacecraft is less than the spacecraft's power consumption and vice versa in the PSM. Energy is stored on the onboard batteries during the PSM and utilised to leverage the mission capabilities during the OM.

The integration of adaptive space subsubsystems and subsystems with other traditional active and passive devices onboard spacecraft for various mission functionalities and/or capabilities has necessitated the re-examination of existing SPSE design procedures. Consequently, an objective investigation of promising spacecraft technologies and the development of a suitable SPSE validation tool that addresses dynamic mission requirements with recourse to post-mission reapplication of space systems are inevitable.

This paper focuses on the design parameters that spacecraft systems engineers can utilise to qualify highly adaptive space systems' capacity, performance and operational time during the pre-launch, mission and post-mission phases. Section II establishes a spacecraft power and energy balance budget for space missions. The multicriteria optimisation of a spacecraft power system with recourse to the METSAT mission is presented in section III. The results and pertinent discussions are stated in section IV. Section V concludes the paper.

II. Spacecraft Power and Energy Budgets

A. Spacecraft Power Estimating Relationships

The design of spacecraft power and energy budgets starts with the identification and qualification of the power consumption requirements of the spacecraft modules of subsystems. The spacecraft power system engineering (SPSE) establishes the power regimes of the various core bus and payload subsystems. Past spacecraft missions have revealed an overwhelming dependency of the total space satellite power on the power consumption requirement of the payload subsystem. Mathematically, the generic total in-orbit power, P_T, of a spacecraft is given by:[1-4]

$$P_T = P_{pl} + P_{cb}(1 + C_f) \qquad (1)$$

where P_{pl} is the payload power consumption (W) P_{cb}, the core bus power consumption (W) and C_f, the power contingency factor. The power margin, P_{margin}, for the spacecraft mission is given by:[1-4]

$$P_{margin} = C_f P_{cb} \qquad (2)$$

For a HASS system with dynamic functional and structural in-orbit operations, Eq. (1) is modified to reflect the varying power requirements that characterise the prevailing respective power modes of the mission. The power mode adjustment takes into account the differential power consumption, δP, occasioned by the dynamic operation and in-orbit onboard processing of a HASS system. The corresponding power margin constraint on Eq. (1) is $P_{margin} \leq P'_{margin} \leq (P_{margin} + \delta P)$.[1] The adaptive power margin function, P'_{margin}, is determined respecting the deterministic and dynamic capability-based mission applications. The total in-orbit power requirement of a HASS system is accurately modelled by:[1-3]

$$P_T = P_{pl} + P_{cb}(1 + C_f) + \delta P \qquad (3)$$

While Eq. (1) defines the total power consumption of the spacecraft subsystems for a minimum payload capability utilisation, Eq. (3) takes into account the maximum capacity and/or data capturing and processing capability of the payload subsystem. Hence, in Eq. (3), the full capacity of the payload module for the designed and emergent missions is envisaged. The differential power variable builds up the satellite power requirement from the static (no-payload or only core bus subsystems utilisation) value to the dynamic (full-capacity payload subsystem) operation level.

Table 1 gives a summary of the mass-based spacecraft power estimating relationships (PERs) for the various categories of small satellites in LEO[2]. Table 2 shows the PERs of the meteorological spacecraft (METSAT) mission. For a 9.2-kg HAN, Table 1 gives the total in-orbit electrical power requirement, P_T, as 24.2 W. This represents the total sunlit solar power (P_{SP}) production of a four-panel solar array. Hence, from Table 2, the minimum power consumption of the payload subsystem for the mission is 12.3 W and the corresponding core bus module's power requirement is 11.9 W.

Table 1. Mass-based spacecraft power estimating relationships in LEO[2]

Satellite category, kg	Power estimating relationship, W
Microsatellite (10 – 100)	$P_T = 1.044M + 15.56$
Nanosatellite (1 – 10)	$P_T = 2.26M + 3.44$
Picosatellites (0.1 – 1)	$P_T = 5M + 0.7$
Femtosatellites (0.01 – 0.1)	$P_T = 10.3M + 0.167$

Table 2. Meteorology spacecraft power estimating relationships in LEO[3]

Satellite category, kg	Power estimating relationship, W
Microsatellite (10 – 100)	$P_T = 0.522M + 0.98P_{pl} + 7.78$
Nanosatellite (1 – 10)	$P_T = 1.13M + 0.98P_{pl} + 1.72$
Picosatellites (0.1 – 1)	$P_T = 2.5M + 0.98P_{pl} + 0.35$
Femtosatellites (0.01 – 0.1)	$P_T = 5.15M + 0.98P_{pl} + 0.0835$

For a C_f of 0.25 and using the nanosatellite's PER in Table 1, we derived the core bus power for a HAN in LEO to be given by:

$$P_{cb} = 1.808M - 0.8P_{pl} + 2.752 \tag{4}$$

The corresponding power margin from Eq. (2) is given by:

$$P_{margin} = 0.452M - 0.2P_{pl} + 0.688 \tag{5}$$

B. Core Bus and Payload Power Consumptions Analysis

For the METSAT mission, four payload subsystems[1,7] are considered; the payloads are paired (P1, P2) and (P3, P4) and their corresponding features are shown in Tables 3 and 4 respectively. The Mitsubishi's camera module[7] features two charged couple chip devices (CCDs) and yields an output image size of 2304 pixel x 1728 pixel.

The total power consumptions for payloads P1, P2, P3 and P4 are 387.6 mW, 717.6 mW, 257.6 mW and 537.6 mW respectively. The spatial resolution of the camera technology; the higher the spatial resolution, the more the power consumed/required during a mission operation. The size (volume) of the satellite represents a key design

parameter for realising the area available for solar panels in the case of a spin-stabilised spacecraft system; for deployable solar panels (in a three-axis stabilised case), the small satellite size mostly dictates the available space for component mounting and integration. Given the common density of 1000 kg/m^3 for the CubeSats, approximately 21cm x 21 cm x 21 cm size is required for the case study 9.2-kg HAN; in an actual mission implementation, these nonconservative size and weight of HAN would be less than the stated values due to the very high level subsubsystems integration (VHLSI).[10,16-19]

Table 3. Payloads 1 and 2 subsystems requirements for the METSAT mission in LEO

Feature	Payload 1 (P1)	Payload 2 (P2)
Sensor technology	OmniVision 2655 CMOS image camera	Mitsubichi's CCD camera module
Sensor power Consumption, mW	250	580
FPGA device	Spartan-3 XC3A400T	Spartan-3 XC3A400T
FPGA power consumption, mW	137.6	137.6
Spatial resolution, pixel	2 x 1024 x 1024	1152 x 864 x 2
Spectral resolution, bit	3 x 8	3 x 8

Table 4. Payloads 3 and 4 subsystems requirements for the METSAT mission in LEO

Feature	Payload 3 (P3)	Payload 4 (P4)
Sensor technology	Sanyo's CCD camera module	Sharp's LZ0P373F CCD camera module
Sensor power Consumption, mW	120	400
FPGA device	Spartan-3 XC3A400T	Spartan-3 XC3A400T
FPGA power consumption, mW	137.6	137.6
Spatial resolution, pixel	1 x 1024 x 1024	1632 x 1224
Spectral resolution, bit	3 x 8	3 x 8

Table 5. Power budget of payload modules for the METSAT mission in LEO

Design Parameter	Payload module			
	P1	P2	P3	P4
Payload module power, W	14.010	14.340	13.880	14.160
Core bus power, W	8.180	7.910	8.280	8.060
Power margin, W	2.040	1.980	2.070	2.010

In this paper, four payload case studies are considered for the METSAT mission. Table 5 is determined based on the maximum individual power consumptions of the subsubsystems (camera and FPGA devices) integrated onto each payload module.

Tables 6 to 9 state the power and/or energy budget of the payloads under consideration. Table 6 reveals that the power margin for each case study payload can be obtained from the range $1.98 \leq P_{margin} \leq 2.04$ W. A 1.2-W Superstar GPS receiver[7] subsubsystem can be integrated onto the HAN system's ADC subsystem for an accurate tracking of at least twelve satellites in its neighbourhood. This promises to enhance a cooperative data relay network thereby virtually increasing the real-time operational times of the downlink and payload processing power modes. Satellites with an accurate neighbour's position can still transmit unfinished transmitted data via a constellation node that has

its footprint coverage on the desired ground station. This would enable an energy budget refinement onboard the satellite system to accommodate the critical data transmission needs outside the temporal window of the communication-overpower (downlink) power mode.

Table 6. Power budget for the METSAT mission in LEO using Payload P1

Subsystem	Power Mode's Power Consumption (W)			
	Power-storing	Communication-overpower	Uplink-overpower	Payload processing-overpower
ADC	0	0	0	0
C&DH	2.500	2.500	2.500	2.500
Uplink	0.750	0.750	0.750	0.750
Downlink	4.580	16.500	16.300	8.300
Payload (camera+FPGAs)	0	5.066	5.066	14.010
Board	0.350	0.350	0.350	0.350
Thermal control	0	0	0	0
Propulsion	0	0	0	0
Mechanics	0	0	0	0
Total	8.180	25.166	24.966	25.910

Table 7. Power budget for the METSAT mission in LEO using payload P2

Subsystem	Power Mode's Power Consumption (W)			
	Power-storing	Communication-overpower	Uplink-overpower	Payload processing-overpower
ADC	0	0	0	0
C&DH	2.500	2.500	2.500	2.500
Uplink	0.750	0.750	0.750	0.750
Downlink	4.310	16.500	16.300	8.300
Payload (camera+FPGAs)	0	5.396	5.396	14.340
Board	0.350	0.350	0.350	0.350
Thermal control	0	0	0	0
Propulsion	0	0	0	0
Mechanics	0	0	0	0
Total	7.910	25.496	25.296	26.240

Table 8. Power budget for the METSAT mission in LEO using payload P3

Subsystem	Power Mode's Power Consumption (W)			
	Power-storing	Communication-overpower	Uplink-overpower	Payload processing-overpower
ADC	0	0	0	0
C&DH	2.500	2.500	2.500	2.500
Uplink	0.750	0.750	0.750	0.750
Downlink	4.682	16.500	16.300	8.300
Payload (camera+FPGAs)	0	4.936	4.936	13.880
Board	0.350	0.350	0.350	0.350
Thermal control	0	0	0	0
Propulsion	0	0	0	0
Mechanics	0	0	0	0
Total	8.282	24.286	24.836	25.780

Table 9. Power budget for the METSAT Mission in LEO using payload P4

Subsystem	Power Mode's Power Consumption (W)			
	Power-storing	Communication-overpower	Uplink-overpower	Payload processing-overpower
ADC	0	0	0	0
C&DH	2.500	2.500	2.500	2.500
Uplink	0.750	0.750	0.750	0.750
Downlink	4.460	16.500	16.300	8.300
Payload (camera+FPGAs)	0	5.216	5.216	14.160
Board	0.350	0.350	0.350	0.350
Thermal control	0	0	0	0
Propulsion	0	0	0	0
Mechanics	0	0	0	0
Total	8.060	25.316	25.116	26.060

C. Orbital Patterns and Operational Time of Spacecraft

Orbital patterns determine the amount of solar power that a satellite captures for the mission. Hence, mission design must incorporate a holistic and objective analysis of the mission requirements vis-à-vis the orbit of deployment. The LEO favours short-term and low-cost missions and most of the small satellite missions have concentrated in the orbit altitude spanning 160 to 2000 km. The inclination and eccentricity of a satellite orbit define the orbital patterns; the inclination defines the angular orbital sweep of a satellite around the Earth relative to the

equator while the eccentricity states the orbit's deviation from an Earth-referenced two-dimensional plane round-trip circle. The orbital pattern parameters form the design variables used to assess the operational and illumination margins and/or regimes of satellites in space. The inclination defines the spatial location of an orbiting satellite relative to the Earth and its range is $0°$ (orbit heading for eastward flight) to $180°$ (orbit heading for westward flight). On the other hand, the eccentricity partitions the orbits into closed (circular and elliptical orbits) and open (hyperbolic and parabolic orbits); open-orbit satellites orbit the Earth once while closed-orbit satellites orbit the Earth periodically along the same path. The METSAT mission reported in this paper will be assessed with recourse to closed orbits.

Small satellites require a nearly constant illumination from the sun for their missions. Sun-synchronous (usually circular and retrograde) orbits spanning 600 to 800 km at $98°$ inclination have been utilised for satellite missions[7]; the satellites experience a nearly constant surface sunlight (illumination) and the daily satellite's ascents and descents over a particular Earth geographic location/latitude occurs at the same local mean time. A sun-synchronous orbit satellite might ascend the Earth ten times a day each time passing over an Earth location at approximately the same local mean solar time. The METSAT images the Earth's landscape in the visible or infrared wavelengths and therefore requires a constant sunlight for its payload's primary mission function and satellite energy supply.

Satellites operating in orbits other than the sun-synchronous experience the Earth's eclipse for a given amount of time during their round-trip. This decreases the available solar energy for the satellite. Mathematically, the eclipse time, t_e, of a satellite is given by:[6]

$$t_e = \frac{\tau_o}{\pi}\left(\cos^{-1}\left(\frac{\sqrt{1-R^2}}{\cos\beta}\right)\right) \tag{6}$$

where,
   R = the radius ratio = R_{eq}/R_{sat}
   R_{eq} = mean equatorial radius of the Earth = 6378 km
   R_{sat} = geocentric radius of the satellite, km = $R_{eq}+H_{sat}$
   H_{sat} = altitude of the satellite, km
   β = Sun-orbit-plane angle, $°$
   τ_o = orbital period of the satellite, s
   μ = gravitational constant of the Earth = 398,600.4418 km^3/s^2

The worst-case β occurs at $0°$ when the satellite experiences the maximum Earth's eclipse and the best-case occurs at $\pm 90°$ when the orbit never enters the Earth's eclipse. The orbital period of the satellite is given by:[6]

$$\tau_o = 2\pi\sqrt{R_{sat}^3/\mu} \tag{7}$$

During the Earth's eclipse, the satellite depends on the onboard storage batteries to maintain system functionalities; the power generation of the solar panels is 0 W while the satellite is eclipsed. Hence, the total energy reserve of the satellite is reduced per an orbital period due to the absence of the Sun's illumination during the eclipse period. The total energy produced by the spacecraft's solar panels, E_o, during a round-trip is given by:

$$E_o = P_{sp}\left(\tau_o - t_e\right) \tag{8}$$

where P_{sp} is the solar panel's average sunlit power generation in a given orbit. This information can be obtained from the datasheets provided by the solar panel manufacturers; a direct practical test of the panels (with recourse to the prevailing space environmental conditions) can also be done. Table 1 provides a summary of the mass-based PER for small satellites utilising a four-panel array in LEO.[1–3,5] The PERs take into consideration the impact of space radiation and other prevailing orbital dynamics that affect the sunlit power generation of solar panels onboard spacecraft in a given orbit.

The sunlit power generation capacity of solar panels is used to develop the electrical energy production of spacecraft in orbits. For a two-power mode system, the following power modes' power consumptions are feasible:
   1) Power-storing, P_s; and

2) Payload processing-overpower, P_p.

The total energy of the spacecraft during a single orbital period for a two-power mode system is given by:

$$E_o = E_s + E_p \qquad (9)$$

where E_s and E_p are the energy consumptions in the power-storing and payload processing-overpower modes respectively. The operational time of the payload processing-overpower mode, t_p, is given by:

$$t_p = \tau_o - \left(t_s + t_e\right) \qquad (10)$$

where t_s is the operational time of the power-storing mode.

From Eqs. (8) and (9), we obtained the operational time of the payload processing-overpower mode for a two-power mode system as:

$$t_p = \frac{E_o - P_s\left(\tau_o - t_e\right)}{P_p - P_s} \qquad (11)$$

Equation (11) can be extended to accommodate several power modes for multiple mission and post-mission applications. For a N-power mode system, the following power consumptions are feasible:
1) Power-storing;
2) Communication (downlink and uplink)-overpower, P_{du}, with a corresponding time, t_{du};
3) Uplink-overpower, P_u, with a corresponding time, t_u;
4) Payload processing-overpower; and
5) Other overpower modes, P_n, with a corresponding time, t_n, where n = 1, 2, …

The energy budget balance for the above in-orbit mission applications is obtained thus:

$$E_o = E_s + E_{du} + E_u + E_p + E_1 + E_2 + ... + E_N \qquad (12)$$

The corresponding operational time of the payload processing-overpower mode is given by:

$$t_p = \tau_o - \left(t_s + t_e + t_{du} + t_u + t_1 + t_2 + ... + t_N\right) \qquad (13)$$

Hence, we derived the in-orbit operational time of the payload processing-overpower mode, t_p, using Eqs. (12) and (13) as:

$$t_p = \frac{E_o - P_s\left(\tau_o - \left(t_e + t_{du} + t_u + t_1 + t_2 + ... + t_N\right)\right) - \left(P_1 t_1 + P_2 t_2 + ... + P_N t_N\right)}{P_p - P_s} \qquad (14)$$

Equation (14) can be re-written thus:

$$t_p = \frac{E_o + P_s\left(\sum_{i=1}^{N-2} t_i + t_e - \tau_o\right) - \left(\sum_{i=1}^{N-2} P_i t_i\right)}{P_p - P_s} \qquad (15)$$

where P_i and t_i represent the ith power mode's power consumption and operational time respectively; the summations in Eq. (15) consider all the power modes except the power-storing and the payload processing-overpower mode. In the case of calculating the operational time of a power mode other than the payload processing-overpower mode's, the latter is held constant and included in the summations while the considered power mode is

9

excluded. The various power modes' power consumptions and their corresponding operational times must be estimated in order to obtain the t_p for the spacecraft mission. Furthermore, the power consumptions of the power-storing mode and the power mode whose operational time is being calculated must be estimated as well.

To maximise the operational time of a power mode, Eq. (15) is adjusted to reflect the maximised power mode. Given the power consumption of the maximised power mode, P_{max}, the corresponding maximised operational time, t_{max}, is obtained from Eq. (15) as:

$$t_{max} = \frac{E_o + P_s(\sum_{i=1}^{N-2} t_i + t_e - \tau_o) - (\sum_{i=1}^{N-2} P_i t_i)}{P_{max} - P_s} \tag{16}$$

Equation (16) is very useful for the multiobjective optimisation of the mission design variables in an integrated design environment. Hence, the operational time of any power mode can be modelled and optimised for a reliable, cost-effective and optimal-performing mission.

III. Multicriteria Optimisation of a Spacecraft Power System

A. Parameter Space Investigation Method

Complex engineering systems such as space-borne equipment require optimised system architectures for their reliability and mission accomplishment. The investigation for optimal solutions generically poses an enormous task of objective locational and procedural searches. The accurate statement of the optimisation problem for the mission and conceptual design objectives enables the feasible solution set and the optimal solutions to be obtained for the space equipment. The parameter space investigation (PSI) method[20] has been created and developed to enable the construction of the feasible solution set for complex engineering systems such as space shuttle, unmanned vehicles, aeroplane, automobiles, ships, control systems, communication network nodes, metallurgical systems, robots and large-scale electrical energy generation systems. The PSI systematically investigates a multidimensional domain space and generates multidimensional points with each point representing a design prototype for the system under development. The PSI method is implemented in the multicriteria optimisation and vector identification (MOVI) software. The integrated PSI-MOVI platform depends on the correct development of the mathematical model governing the complex engineering system under investigation. An approximate model of any engineering system is also supported by the PSI-MOVI application. The tools for constructing and analysing the feasible solution set of a multicriteria optimisation problem are provided by the PSI method and the MOVI system.[20]

The PSI method enables the identification, optimisation and analysis of constraints on design variables, functional dependencies and multicriteria; these constitute the feasible solution set of the optimisation problem. The method comprises three major stages: compilation of test tables, selection of criterion constraints and verification of the solvability of the optimisation problem.[20]

B. Multicriteria Design of Spacecraft Power System

In this paper, we applied the PSI method in the multicriteria design of the spacecraft power system engineering for small satellites in LEO. The mathematical model of the electrical power requirement of the spacecraft modules was developed based on past missions and emerging space systems technology. We placed an objective emphasis on the spacecraft design variables that occasion dynamic, cost-effective and reliable operations with recourse to post-mission applications. A METSAT mission in LEO was chosen as the candidate small satellite mission. We limited the scale of the optimisation problem to three design variables: the payload power, P_{pl}, total spacecraft power, P_T and mass contingencies, M. We developed four functional constraints and six criteria parameters respecting the candidate METSAT mission. The functional and criteria constraints were set to minimise the total power consumptions of the HAN and its payload. The in-orbit dry mass was also minimised in the optimisation problem. The results of the multicriteria optimisation of the SPSE design are stated in section IV.

IV. Results and Discussions

A. Orbital and Operational Times

Table 10 shows the orbital patterns[6] that we utilised to investigate the appropriateness of payloads P1 to P4 for the METSAT mission with recourse to the in-orbit power budget and operational times. The orbit, inclination and altitude were chosen according to reflect the typical prevailing operational orbital margins of small satellite missions

in LEO.[5–7] The suitability of each orbit for the mission was also considered based on the average energy production per orbital period and the desired data rates for the downlink communication. For the METSAT mission, we evaluated the power and energy budget by setting the uplink and downlink operational times to 10 minutes respectively. The communication-overpower mode utilizes 10 minutes for both the communication-downlink-overpower and communication-uplink-overpower modes. Tables 11 to 14 show the operational times for the payloads P1 to P4; the analyses were done using Tables 5 to 10 and Eq. (15). The operational times of the payload processing-overpower mode, t_{pp1} to t_{pp4}, for each candidate payload were obtained with recourse to the average eclipse time per orbit and altitude of deployment (Table 10).

Table 10. Orbital patterns for the METSAT Mission in LEO

Orbit	H_{sat}, km	β range, °	τ_o, mins	t_{eavg}, min
Equatorial	300	-23:23	90.5	36.2
Inclination 22.5	400	-43:45	92.6	35.2
Inclination 45	500	-61:65	94.6	32.7
Inclination 67.5	600	-88:85	96.7	26.1
Inclination 90 (polar)	300	36:60	90.5	32.3
Inclination 112.5	400	-88:88	92.6	29.7
Inclination 135	500	-67:63	94.6	32.6
Inclination 157.5	600	-46:46	96.7	34.3
Inclination 180	800	-23:23	100.9	34.4
Sun-synchronous (polar) 90	300	71:79	100.9	0
Sun-synchronous (nonpolar) 98	400	-75:82	92.6	0

Table 11. Operational times of the candidate payloads for the METSAT Mission in LEO

Orbit	H_{sat}, km	t_{pp1}, min	t_{pp2}, min	t_{pp3}, min	t_{pp4}, min
Equatorial	300	30.02	28.49	30.79	29.63
Inclination 22.5	400	32.82	31.18	33.61	32.41
Inclination 45	500	36.88	35.09	37.70	36.44
Inclination 67.5	600	44.74	42.64	45.62	44.24
Inclination 90 (polar)	300	33.54	31.87	34.34	33.12
Inclination 112.5	400	37.79	35.95	38.61	37.33
Inclination 135	500	36.97	35.17	37.80	36.53
Inclination 157.5	600	37.33	35.52	38.16	36.89
Inclination 180	800	41.04	39.08	41.89	40.57
Sun-synchronous (polar) 90	300	72.12	68.96	73.18	71.41
Sun-synchronous (nonpolar) 98	400	64.62	61.75	65.63	63.97

Table 10 shows that the orbital period of as spacecraft is largely dependent upon the orbital pattern chosen for the mission. Sun-synchronous orbits favour the small satellite missions for its near-constant sunlight and relatively high round-trip duration for the 90 ° polar orbit; an orbital spacecraft experiences no eclipse. At an altitude of 800 km and inclination of 180 °, the HAN system would experience an average eclipse time of 34.4 minutes.

Table 12. Excess energy storage for the METSAT Mission in LEO

Orbit	H_{sat}, km	E_{ep1}, Wh	E_{ep2}, Wh	E_{ep3}, Wh	E_{ep4}, Wh
Equatorial	300	1.73	2.35	1.42	1.88
Inclination 22.5	400	1.85	2.51	1.53	2.01
Inclination 45	500	2.02	2.75	1.69	2.20
Inclination 67.5	600	2.36	3.21	2.01	2.56
Inclination 90 (polar)	300	1.88	2.55	1.56	2.05
Inclination 112.5	400	2.06	2.80	1.73	2.24
Inclination 135	500	2.03	2.75	1.70	2.21
Inclination 157.5	600	2.04	2.77	1.71	2.22
Inclination 180	800	2.20	2.99	1.86	2.39
Sun-synchronous (polar) 90	300	3.54	4.81	3.11	3.83
Sun-synchronous (nonpolar) 98	400	3.22	4.38	2.81	3.48

While the sun-synchronous orbits remain the favoured for the METSAT mission, Table 11 reveals that at 800 km altitude and 180 $^\circ$ inclination, an average of 40 minutes for the operational times of the candidate payloads under investigation is obtained. This leaves the choice of the appropriate payload to be considered based on the desired data quality and integrity and the expected system performance. In a typical spacecraft mission, more operational time is required for the payload subsystem. Table 12 states the excess energy stored during the METSAT mission as the spacecraft orbits around the Earth. As expected, the sun-synchronous orbits store the most energy for each payload configuration. At 800 km altitude and 180 $^\circ$ inclination, the HAN system stores an average of 2.4 Wh. Thus, the energy budget balance reveals that a polymer Li-ion battery with a capacity of 3.99 Wh can store the round-trip excess energy for an increased operational time for the payload processing-overpower mode. During the eclipse time, the payload and an active thermal subsystem can be accommodated. Furthermore, the analysis indicates that a low-cost three-axis momentum wheel with an accuracy of <0.01 $^\circ$ can be integrated with a moderate difficulty; this would utilise attitude sensors which can be conveniently supported by the HAN system.

The excess energy stored, E_{ep} on the batteries per orbital period and based on the operational times of the individual payloads are summarised in Table 12. The minimum storable excess energy is 1.42 Wh and the maximum, 4.81 for the considered candidate payloads. Including two polymer Li-ion batteries in the electrical power subsystem of the HAN, each with a capacity of 3.89 Wh, would enable secondary payloads and more operational times for a power mode of interest to be accomplished for the METSAT mission.

B. Data Transmission

Data transmission from a spacecraft to a ground station is inevitable for any given space mission. The operational times of the communication-overpower mode and the data rate of the downlink greatly influence the data delivery to a ground station. For a 9600 bps data rate and downlink time of 10 minutes, 720 kB of data can be transmitted to a ground station. If this is increased to 19200 bps, 1440 kB of data can be downlinked. The challenge lies in the spatial and spectral resolutions of the payload module onboard the spacecraft and the data quality expected by the end-user. A payload with a sensor (camera) of 2-Mpixel spatial resolution and 3 x 8 bits spectral resolution would generate a data size of approximately 6.3 MB. If the HAN system transmits at 9600 bps, only about 11.4 % of the payload data would be transmitted within 10 minutes of its contact with a ground station. The 19200 bps data rate allows the HAN system to downlink 22.9 % of its payload data to a ground station within its footprint. Increasing the data rate to 100 kbps enables the HAN system to downlink approximately 7.5 MB to a 4-m diameter ground station antenna during its 10 minutes pass. This would completely transmit the data generated by payloads P1, P3 and P4 and about 60 % of the data generated by payload P2. A second approach would be to implement a JPEG (joint pictures expert group) compression algorithm on the onboard signal processing devices such as FPGAs. This would allow the payload data to be transmitted to the ground station at the expense of some information. The JPEG algorithm scales the data to be transmitted to fit the allowable maximum data size of the downlink (data link) margin. For a 4-Mpixel image, the unprocessed data size is 12.58 MB. The corresponding

compression ratio at 100 kbps downlink margin is 1: 1.68. This is well below the allowable maximum compression ratio of 1:10.[7] Hence, the HAN system can still process its payload data within its payload's operational time of 40 minutes and downlink a good quality data to a ground station within 10 minutes.

C. Multicriteria Optimisation of the HAN Power System Engineering

The results of the multicriteria optimisation of the HAN power system engineering is shown in Figures 1 to 5. The design variables for the SPSE optimisation problem were the mass of HAN, the payload power consumption and the power contingency. Figure 1 states the optimisation vectors of the HAN system's SPSE design. The pareto optimal solution concentrates around 9.2 kg for the METSAT mission implementation. It shows the histogram of the feasible and pareto optimal solutions for the first design variable (mass of HAN) for the METSAT mission.

Figure 2 shows the optimisation design vectors that represent the histogram of the feasible and pareto solutions set for the second design variable (payload power) for the METSAT mission. The pareto optimal solution for the baseline power consumption of HAN's payload module is indicated by the green dots. These power consumptions are the minimum that can sustain the METSAT mission given the mission and conceptual design objectives. The optimisation result yielded 12.36 W as the best (minimum) baseline payload module power consumption for the mission. The corresponding core bus power consumption and power margin for the mission were obtained from the multicriteria optimisation as 9.5 W and 2.37 W respectively.

Figures 3 and 4 indicate that the optimised payload power consumption for the METSAT mission is 12.36 W. This forms the design point in the choice of the components of the payload module for the mission. The stated power is based on the minimum acceptable data capturing, processing and transmission quality for the mission. In Fig. 3, the total payload power consumption is compared with the HAN category that can satisfy the mission and conceptual design objectives. Figure 4 reports the entire optimisation solutions set for the total HAN power requirement and the corresponding payload power consumption. The histogram of the feasible and pareto optimal solutions for the third design variable (contingency factor) are given in Fig. 5. The power margin versus contingency factor graph is shown in Fig. 6. The pareto optimal solutions for the HAN system yielded a power margin of 2.37 W; this is approximately 10 % of the total spacecraft power and satisfies the stipulated mission's conceptual design requirement.[4] It is required for the mission to have enough power margin for emergent capabilities and operational uncertainties; Figs. 5 and 6 were obtained for a minimised power margin design to enable the threshold power margin for the mission to be determined. The performances of the design variables are further explained in the optimisation criteria for the METSAT mission (Fig. 7). Six criteria were considered by the authors and the results indicate the worst and best results realisable for the METSAT mission.
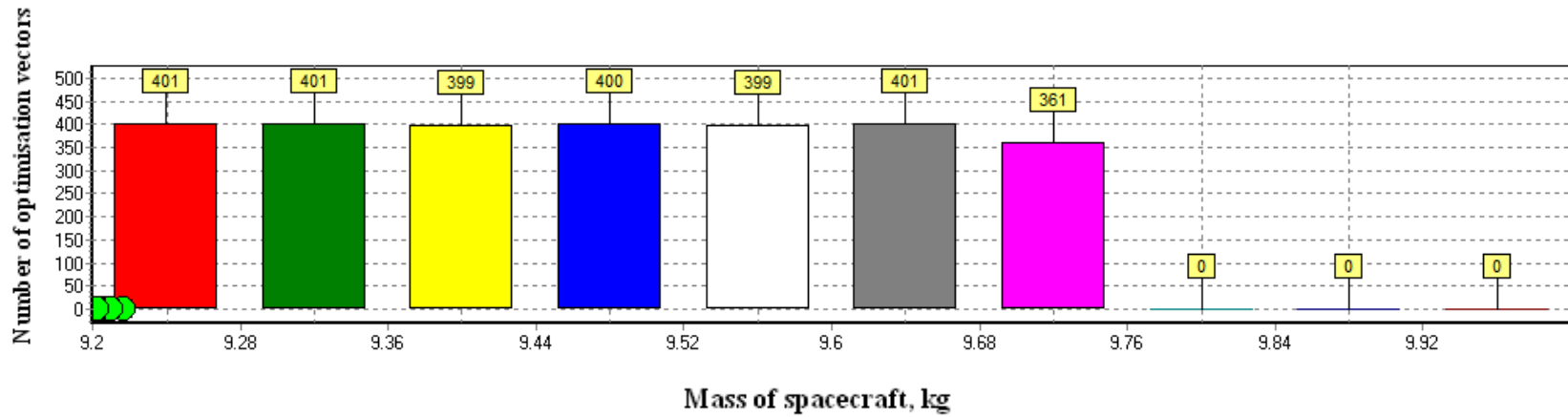
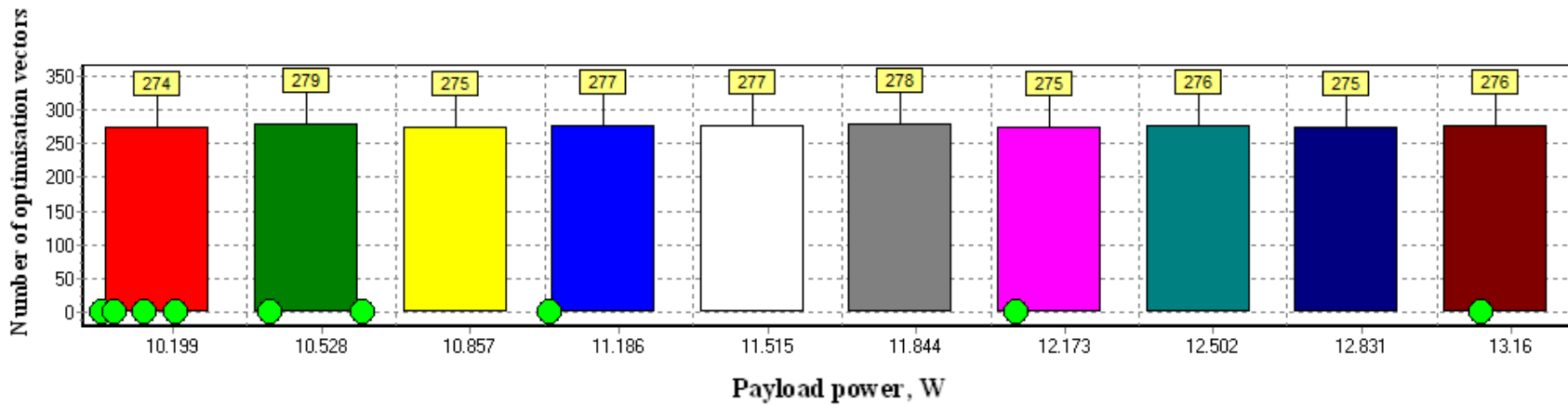**Figure 1. Optimisation vectors versus mass of spacecraft for the METSAT mission**

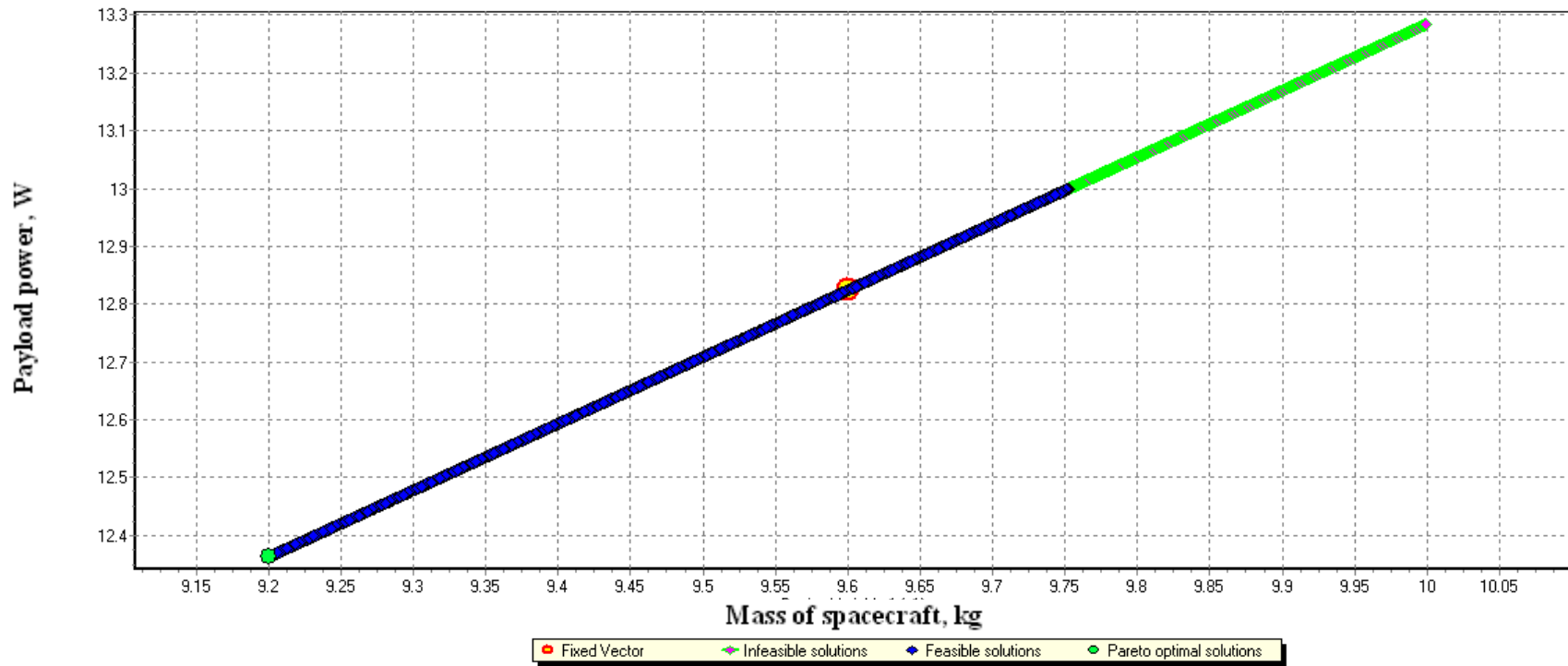**Figure 2. Optimisation vectors versus payload power for the METSAT mission**

Figure 3. Optimised payload power versus mass of spacecraft for the METSAT mission
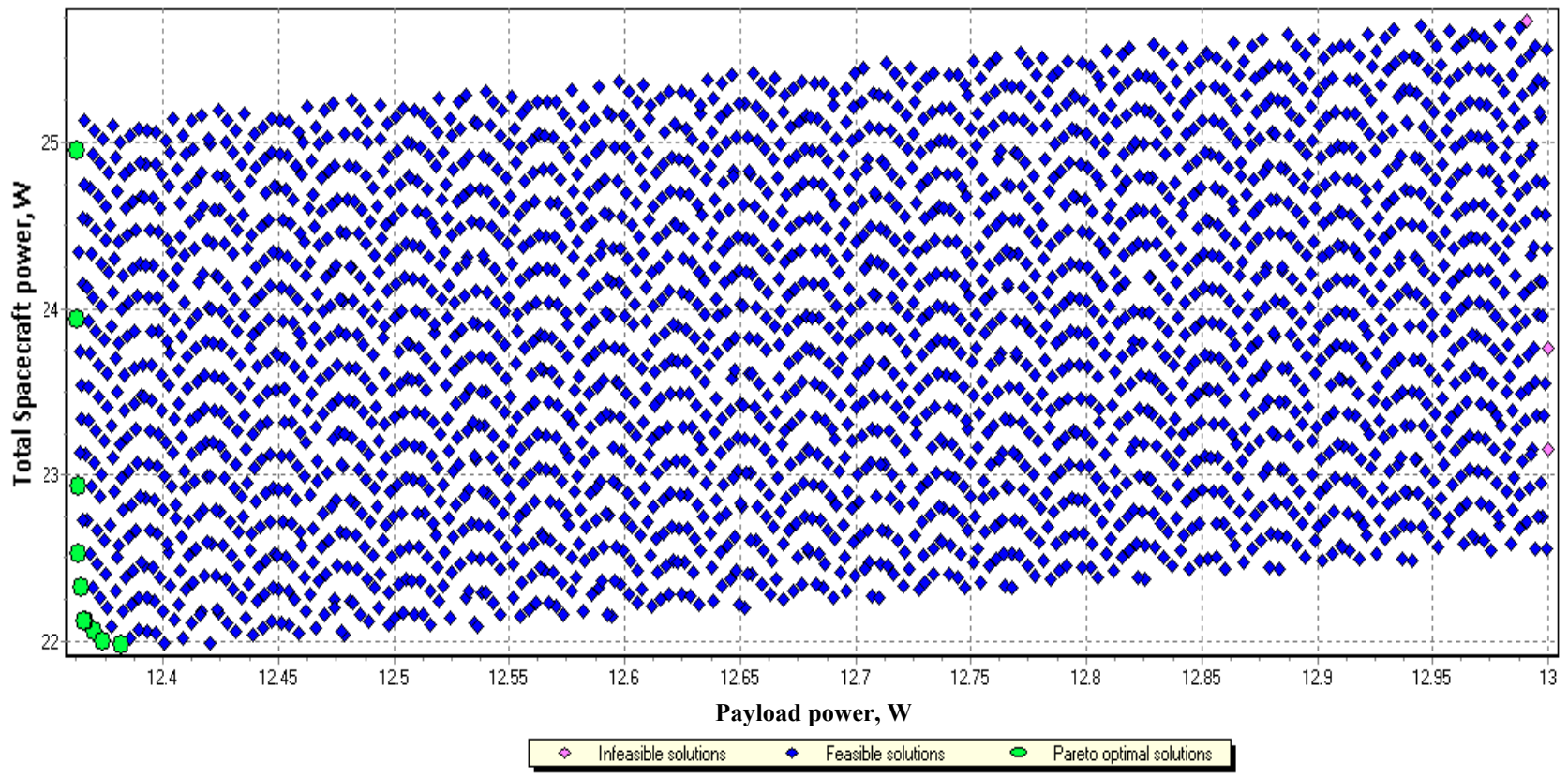
American Institute of Aeronautics and Astronautics

Figure 4. Optimisation solutions set of the total spacecraft and payload power consumptions
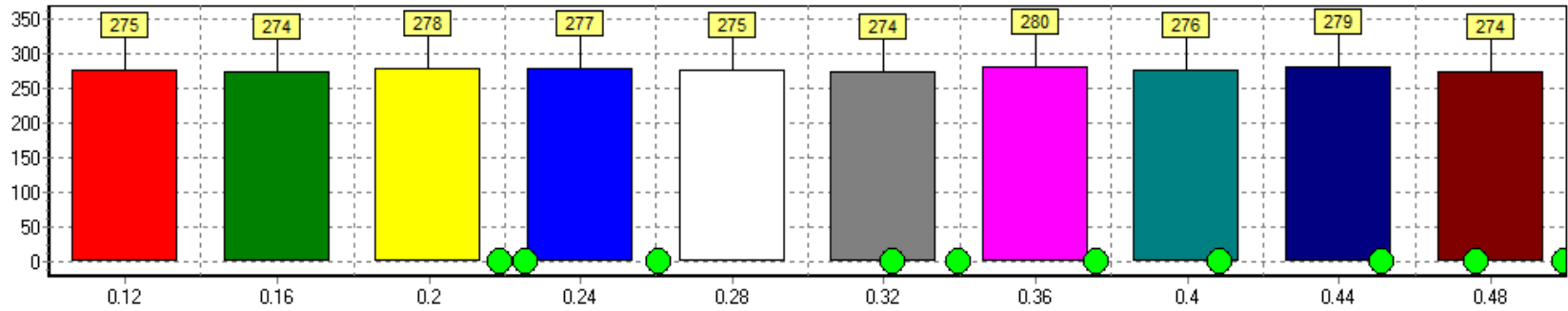
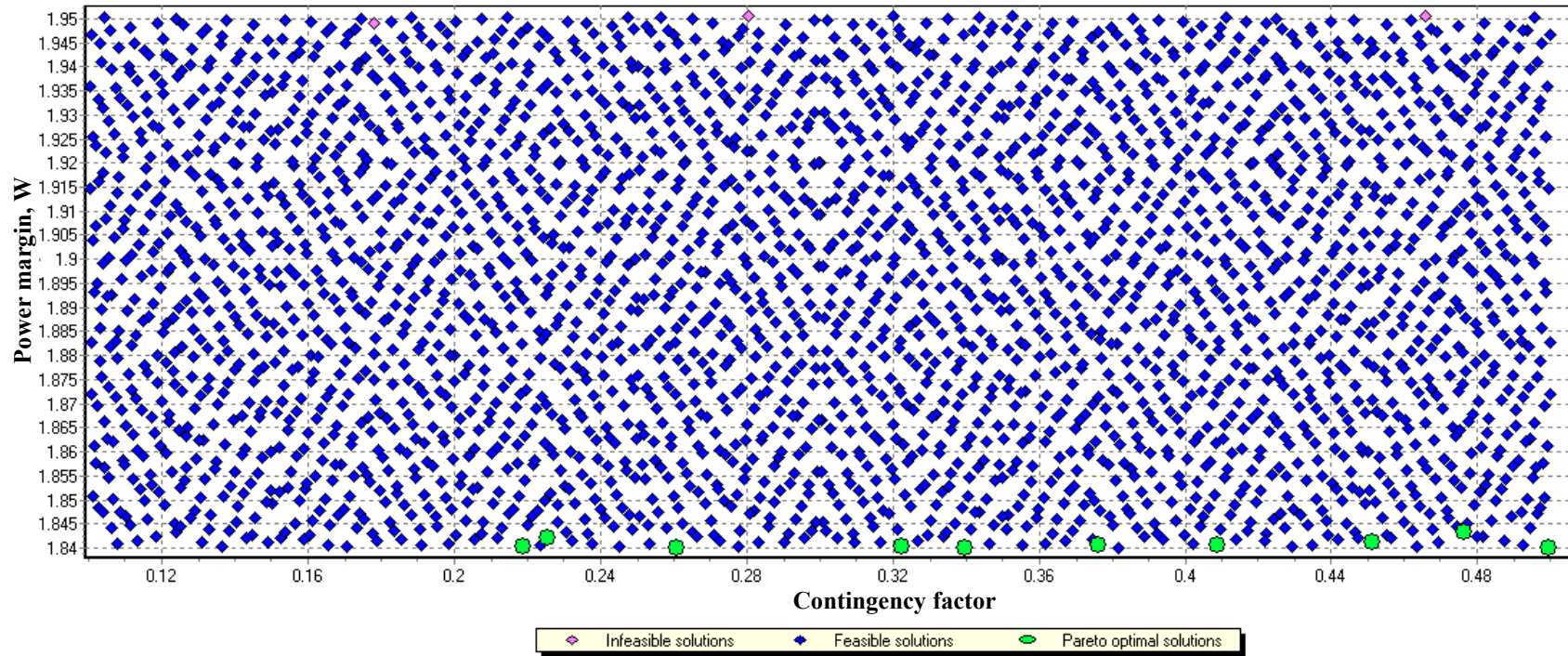**Figure 5. Optimisation vectors versus power contingency for the METSAT mission**

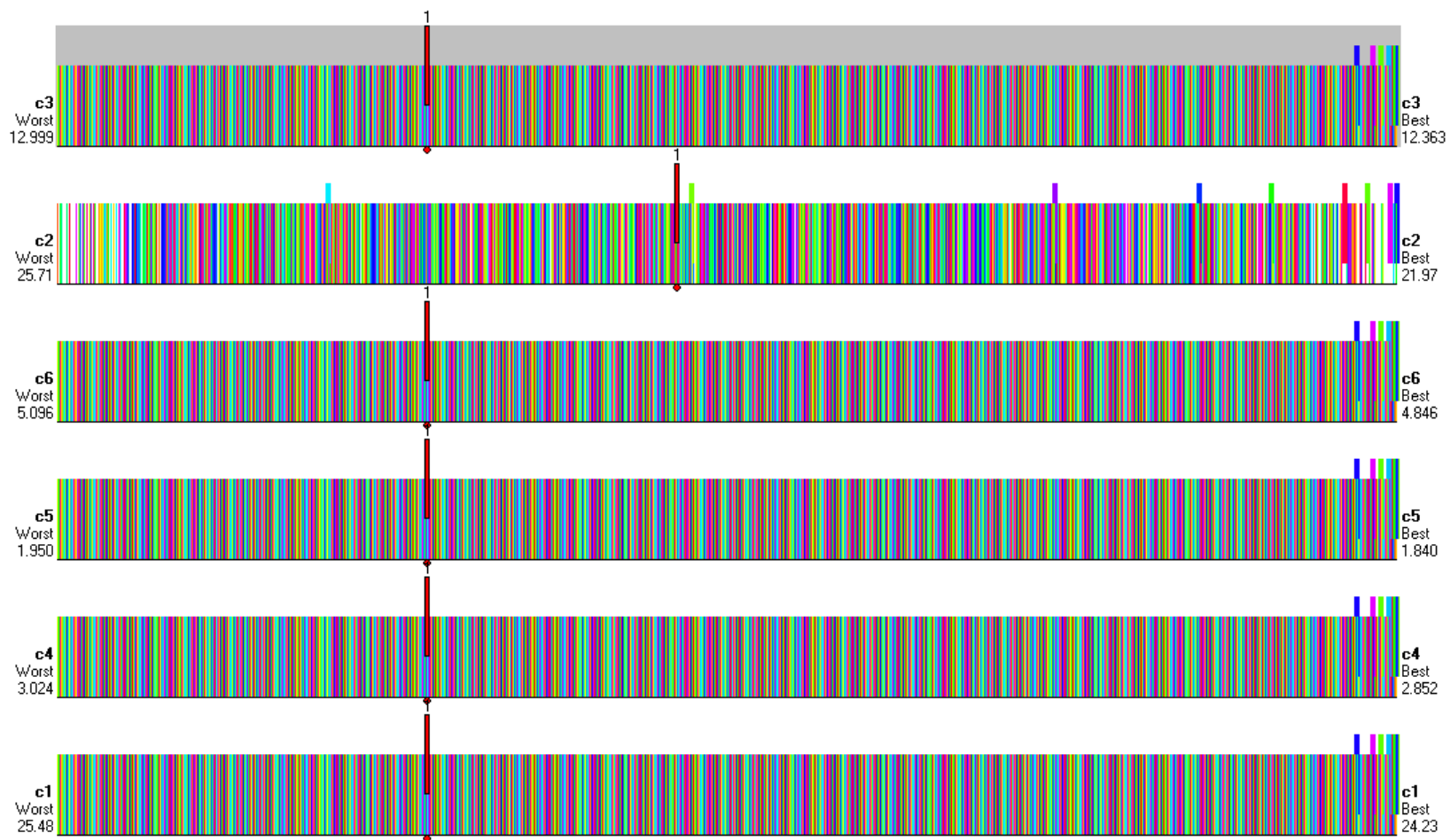**Figure 6. Optimisation solutions set of the power margin and contingency factor**

Figure 7. Optimisation criteria for the METSAT mission's design variables

American Institute of Aeronautics and Astronautics

V. Conclusion

A multicriteria optimisation of a highly adaptive nanosatellite system has been investigated and reported in this paper. Four candidate payload modules, each containing a camera and an FPGA device, were chosen for a meteorology mission. The multicriteria optimisation yielded a 9.2-kg HAN for the METSAT mission. We carried out an analysis of the orbital patterns and the operational times of the 9.2-kg HAN. Furthermore, the authors calculated the total energy production of the HAN system at an altitude of 800 km and inclination of 180 $^{\circ}$ as 26.82 Wh. The operational time of 40 minutes for the payload processing-overpower model and downlink time of 10 minutes are well suited for the mission. The HAN system also received uplink engineering data for 10 minutes during its orbital period. The reported power and energy balance budget for the METSAT mission using a highly adaptive small satellite promises to enable spacecraft systems engineers objectively and reliably design, validate and develop spacecraft mission assets with economies of scale.

Acknowledgments

References

[1]Ekpo, S., and George, D., "A System Engineering Analysis of Highly Adaptive Small Satellites," *IEEE Systems Journal*, Vol. PP, No. 99, 2012, pp. 1–8.

[2]Ekpo, S., and George, D., "A Power Budget Model for Highly Adaptive Small Satellites," *Recent Patents on Space Technology*, Vol. 3, No. 2, 2013, pp. 1–9.

[3]Ekpo, S., and George, D., "A System Engineering Consideration for Future-Generations Small Satellites Design," *Proceedings of the First IEEE European Satellite Telecommunications Conference*, Rome, 2012, pp. 1–4.

[4]Brown, C., *Elements of Spacecraft Design*, AIAA, Inc., Virginia, 2002, pp. 1–43.

[5]Janson, S. W., *"The Future of Small Satellites," Small Satellites: Past, Present, and Future*, edited by Helvajian, H., and Janson, S. W., AIAA, Inc., Virginia. pp. 771–810, 2008.

[6]Arnold, S. S., Nuzzaci, R., and Gordon-Ross, A., "Energy Budgeting for CubeSats with an Integrated FPGA," *IEEE Aerospace Conference*, Big Sky, Montana, 2012, pp. 1–14.

[7]P. Mario, "Study of a Cube-Sat Mission," University of Karl Franzens University of Graz, Austria, 2005, pp. 56–82.

[8]Ekpo, S., and George, D., "A System-based Design Methodology and Architecture for Adaptive Small Satellites," *Proceedings of the 4th Annual IEEE International Systems Conference,* San Diego, CA, 2010, pp. 516–519.

[9]H.Schmitz , "Application Examples: How to Use FPGAs in Satellite Systems," *Actel Corporation, California*, 2010, pp. 1–7.

[10]Ekpo, S., and George, D., "A Deterministic Multifunctional Architecture Design for Highly Adaptive Small Satellites," *International Journal of Satellite Communication Policy and Management*, Vol.1, No.2/3, 2012, pp. 174–194.

[11]J. Saleh, D. Hastings, and D. Newman, "Spacecraft Design Lifetime," *Journal of Spacecraft and Rockets,* Vol. 39, No. 2, 2002, pp. 244–257.

[12]Vladimirova, T. and Barnhart, D. J., *"Towards Space-based Wireless Sensor Networks," Small Satellites: Past, Present, and Future*, edited by Helvajian, H., and Janson, S. W., AIAA, Inc., Virginia. pp. 595–629, 2008.

[13]Ekpo, S., and George, D., "Impact of Noise Figure on a Satellite Link Performance," *IEEE Communications Letters*, Vol. 15, No. 9, 2011, pp. 1–3.

[14]Ekpo, S., and George, D., "4–8 GHz LNA design for an adaptive small Satellite Transponder using InGaAs PHEMT Technology," *Proceedings of the 11th IEEE Wireless & Microwave Conference*, Melbourne, FL, 2010, pp. 1–4.

[15]Ekpo, S., and Kettle, D., "Mm-wave LNAs design for adaptive small Satellite applications," *Proceedings of the Joint 5th ESA Workshop on Millimetre Wave and 31st ESA Antenna Workshop*, Noordwijk, Netherlands, 2009, pp. 843–847.

[16]Barnhart, D., Vladimirova, T., and M. Sweeting, "Very-Small-Satellite Design for Distributed Space Missions," *Journal of Spacecraft and Rockets,* Vol. 44, No. 6, 2007, pp. 244–257.

[17]Ekpo, S., and George, D., "Reconfigurable Cooperative Intelligent Control Design for Space Missions," *Recent Patents on Space Technology*, Vol. 2, No. 1, 2012, pp. 2–11.

[18]B. Jackson and K. Epstein, "A Reconfigurable Multifunctional Architecture Approach for Next Generation Nanosatellite Design," *Proceedings of the IEEE Aerospace Conference, Vol.7, 2000*, pp. 185–188.

[19]Ekpo, S., and George, D., "A Highly Adaptive Small Satellites Experiment for Space Missions Modelling," *International Journal of Satellite Communication Policy and Management*, Vol. 2, 2013, pp. 1–18.

[20]Statnikov, R., and Statnikov, A., "The Parameter space Investigation Method," Artech House Publishers, Inc., London, 2011, pp. 13–94.